Supplementary Materials

Materials and Methods

Pulmonary Function: Lung mechanics were assessed in anesthetized mice using the flexiVent mechanical ventilator system (SCIREQ, Montreal, PQ, Canada) as previously described (1). Mice were anesthetized with ketamine/xylaxine/acepromazine i.p., tracheostomized with a 20-gauge luer stub (Insetech, Plymouth Meeting, PA), and connected to the flexiVent. Mechanical ventilation was set at 150 breath/minute with tidal volume of 0.16 ml/kg. Lung mechanics including airway resistance, airway elastance, compliance, tissue elastance, and tissue damping were measured.

Immunoblots: Whole lungs were homogenized in PBS containing protease inhibitor cocktails. Protein (30μg) was analyzed by SDS-PAGE/Western blot under non-reduced (SP-B) and reduced (SP-C) conditions with antibodies against mature SP-B (1:5,000; WRAB-48604; Seven Hills Bioreagents), mature SP-C (1:15,000; WRAB-76694; Seven Hills Bioreagents), and a loading control GAPDH (1:10,000; A300-641A; Bethyl Laboratories).

Proteomics analysis: BALF proteins were extracted as previously described (2). Isolated BALF proteins were denatured, alkylated, digested with trypsin and desalted on a C18 SPE cartridge as previously described (2). Peptides were evaluated by LC-ESI-MS/MS using a Waters nanoACQUITY UPLC system interfaced with a Q Exactive mass spectrometer (Thermo Scientific, San Jose, CA). The LC-MS/MS system for proteomics was as previously described (2). Mass spectrometric raw data were analyzed in MaxQuant, version 1.5.2.8. with a false discovery rate set at 0.01(3). Proteins were identified with at least 2 peptides by searching against the Mus

musculus Uniprot database (UniprotKB, downloaded in 2015). Carbamidomethylation was set as fixed modification and N-terminal acetylation and oxidation of methionine were included as dynamic modifications. LFQ quantification (4) was used for protein quantification.

Morphometric analyses: Nikon Elements 4.50 was used to calculate the width and mean chord length of alveolar walls. RGB General Analysis algorithms were created using HSI mode. All images were white balanced by auto contrast to ensure all white airspaces were excluded from acceptance into the alveolar wall. In HIS mode, all hues (H, 0-255) and saturations (S, 0-255) were accepted allowing all colors to be included in the alveolar wall space. Only high intensities were excluded by selecting intensities from 0-215, eliminating airspaces from calculated data. Alveolar width is defined as the distance across the alveolar wall and mean chord length is calculated by the area/mean secant length.

Supplementary References

1. Kramer EL, Mushaben EM, Pastura PA, Acciani TH, Deutsch GH, Khurana Hershey GK, et al. Early growth response-1 suppresses epidermal growth factor receptor-mediated airway hyperresponsiveness and lung remodeling in mice. *Am J Respir Cell Mol Biol*. 2009;41(4):415-25.
2. Dautel SE, Kyle JE, Clair G, Sontag RL, Weitz KK, Shukla AK, et al. Lipidomics reveals dramatic lipid compositional changes in the maturing postnatal lung. *Scientific reports*. 2017;7:40555.
3. Cox J, and Mann M. MaxQuant enables high peptide identification rates, individualized p.p.b.-range mass accuracies and proteome-wide protein quantification. *Nat Biotechnol*. 2008;26(12):1367-72.
4. Cox J, Hein MY, Luber CA, Paron I, Nagaraj N, and Mann M. Accurate proteome-wide label-free quantification by delayed normalization and maximal peptide ratio extraction, termed MaxLFQ. *Molecular & cellular proteomics : MCP*. 2014;13(9):2513-26.

Supplementary Figures and Tables:

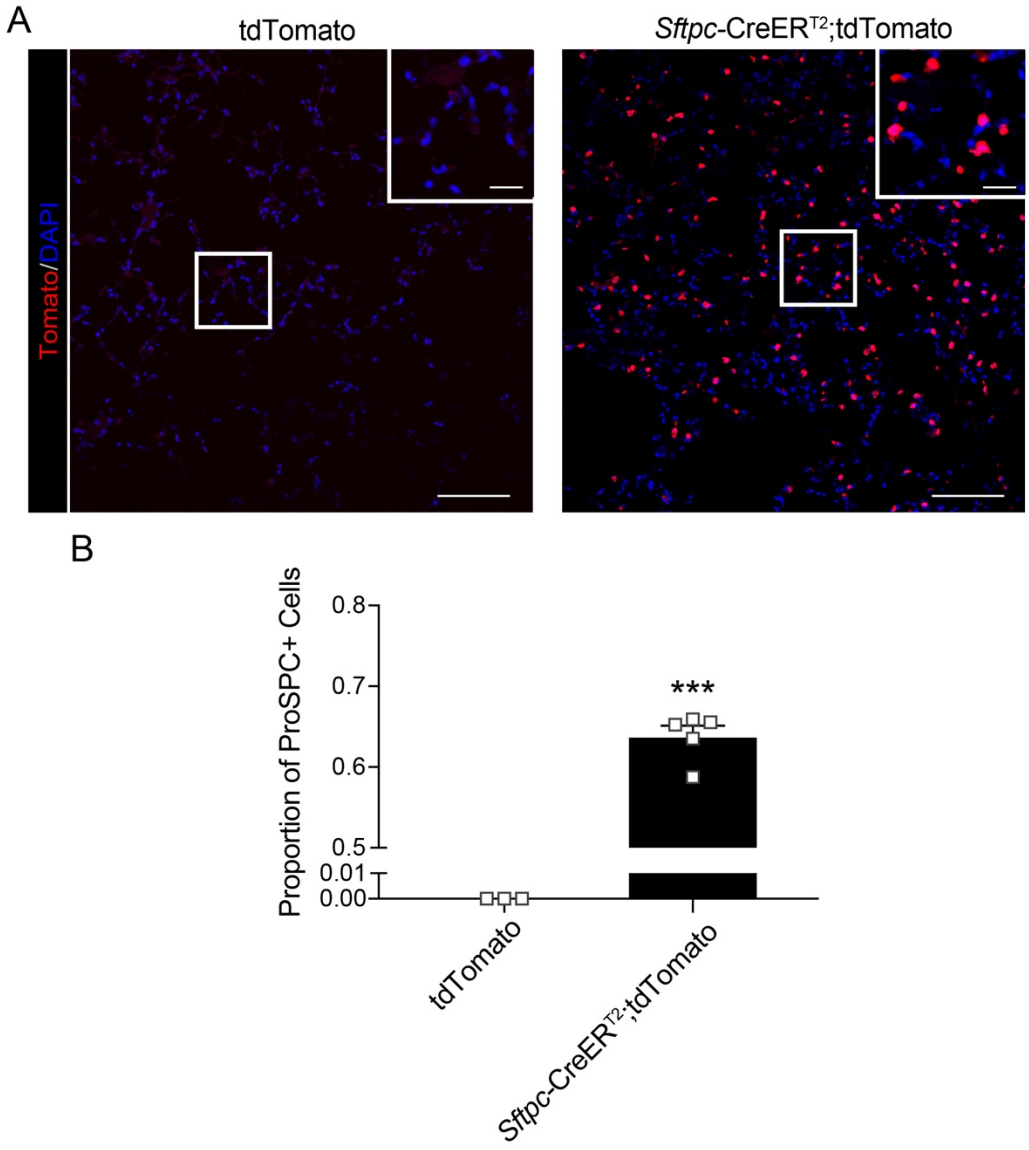

Fig. S1. Spontaneous recombination and labeling in *Sftpc*-CreER^{T2} mice. A) Representative immunofluorescence images show tdTomato (red) and DAPI (blue) in frozen lung sections of Gt(ROSA)26Sor^{tdTomato} (tdTomato) mice and *Sftpc*-CreER^{T2};Gt(ROSA)26Sor^{tdTomato} (*Sftpc*-CreER^{T2};tdTomato) mice in the absence of tamoxifen. Scale bars = 100 μm, inset scale bars =20 μm. **B)** Tomato^{+}, proSPC^{+} cells were quantitated using Nikon Elements General Analysis software

in tdTomato and *Sftpc*-CreER^{T2};tdTomato mice in the absence of tamoxifen. Bars represent mean ± SE, n=3-5/group, ***p=0.0004 compared to tdTomato as determined by one-way ANOVA.

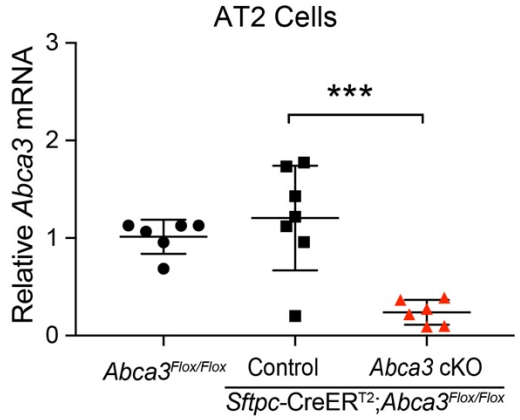

Fig. S2. Deletion of ABCA3 in AT2 cells. *Abca3* mRNA was measured by RT-PCR in purified AT2 cells from *Abca3*$^{flox/flox}$ and untreated or tamoxifen treated *Sftpc*-CreER^{T2};*Abca3*$^{flox/flox}$ (control and *Abca3* cKO) mice following 6 days of tamoxifen with an exon 3-4 probe, normalized to *β-actin*. Data are mean ± SE, n=6-7/group, ***p=0.0004 as determined by one-way ANOVA.

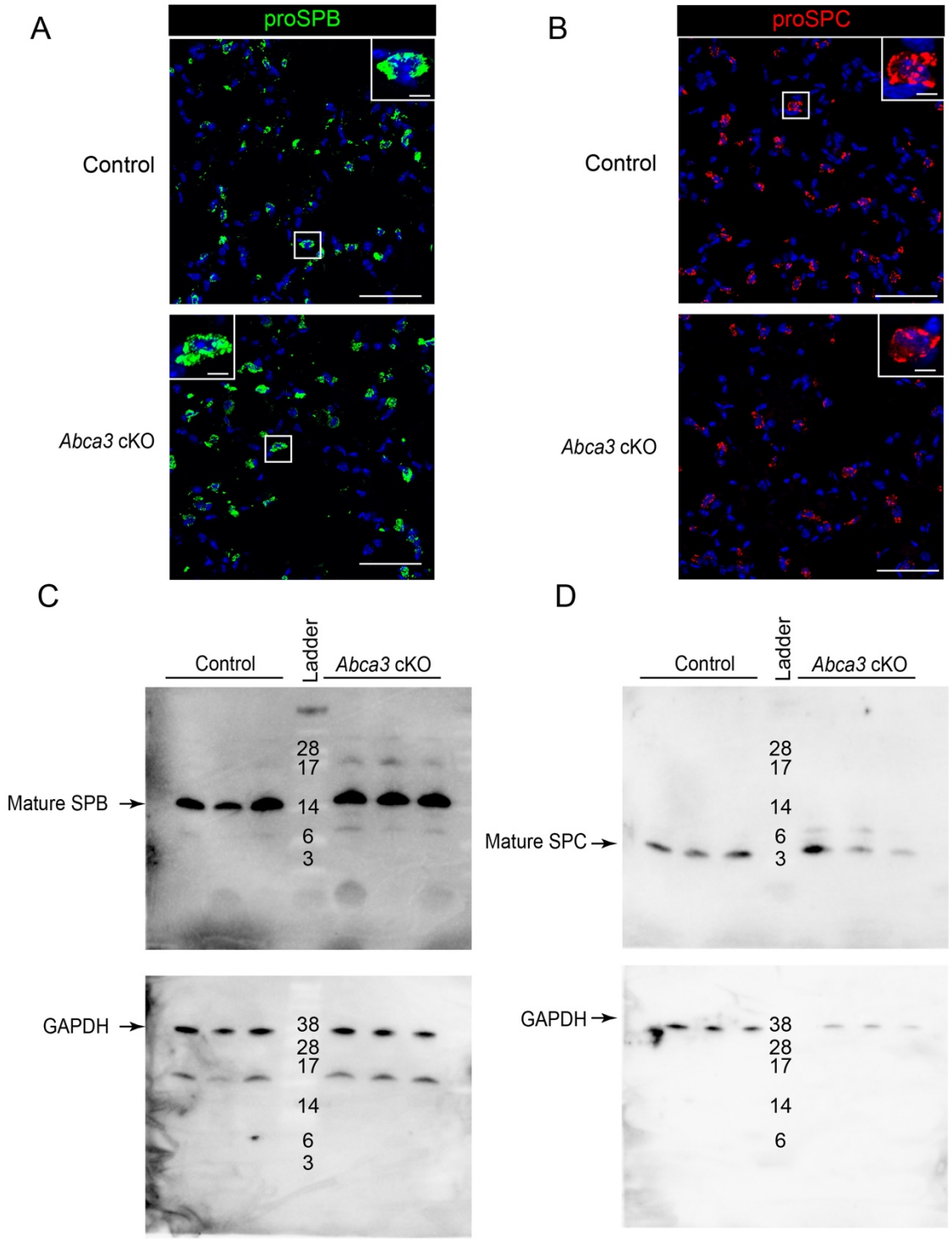

Fig. S3. ABCA3 is not required for normal processing of surfactant-associated proteins.

Representative immunofluorescence images of proSPB (green, **A**) and proSPC (red, **B**) in control

and *Abca3* cKO lungs treated with tamoxifen for 11 days. Scale bars = 50 μm, inset scale bars = 5 μm. Immunoblots for mature SPB (**C**) and mature SPC (**D**) from whole lung lysates of control and *Abca3* cKO mice treated with tamoxifen for 6 days. GAPDH served as a loading control, n=3 mice/group.

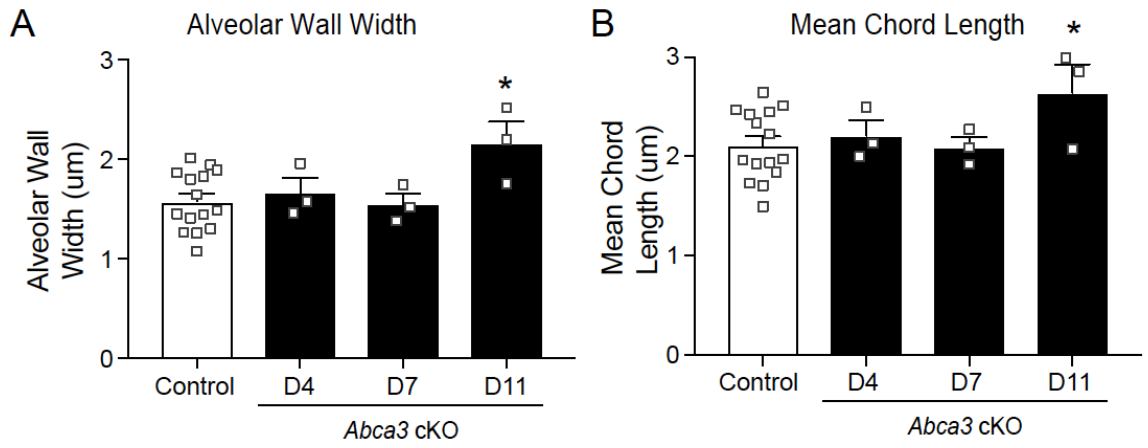

Fig. S4. Deletion of ABCA3 causes alveolar wall thickening. Alveolar wall dimensions were quantified in control and *Abca3* cKO mice after 4, 7 and 11 days of tamoxifen as alveolar wall width (**A**) and mean chord length (**B**) using Nikon Elements General Analysis software. Data are mean ± SE, n=3-15/group, *p=0.01 as determined by one-way ANOVA. Representative images are shown in Figure 1.

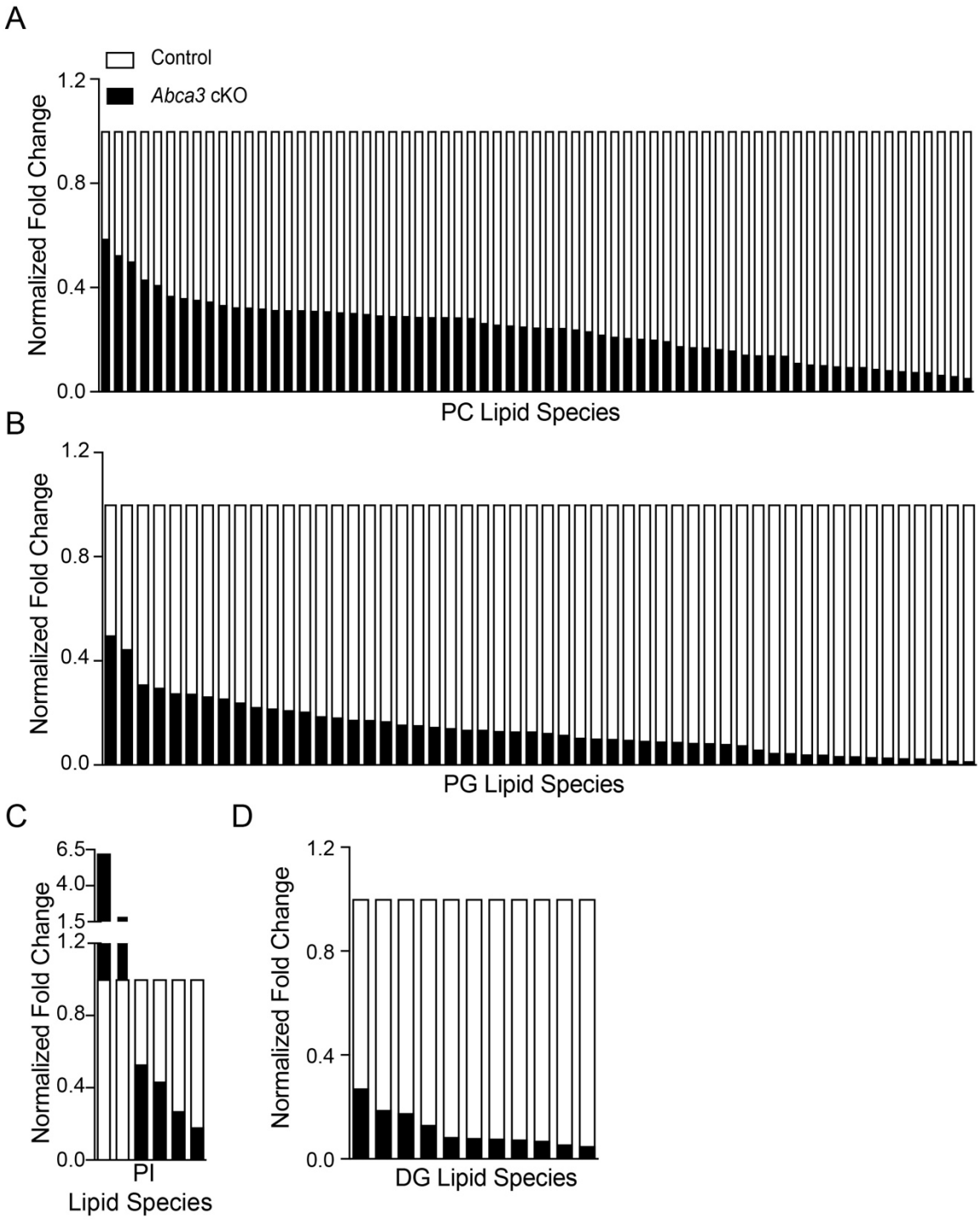

Fig. S5. Decreased phospholipids after deletion of *Abca3* in AT2 cells. BALF was collected from control and *Abca3* cKO mice treated with tamoxifen for 7 days for lipidomic analysis as described in the methods. Phosphatidylcholine (PC, **A**), phosphatidylglycerol (PG, **B**),

phosphatidylinositol (PI, **C**), and diacylglycerol (DG, **D**) species were determined by mass spectrometry as described in the methods. Control (open bar) and *Abca3* cKO (closed bar) are superimposed for each lipid species normalized to fold change (**Supplemental Table S1** lists the corresponding fold changes for individual lipid species). Significant changes in lipid species have a $p<0.01$, fold change >1.2.

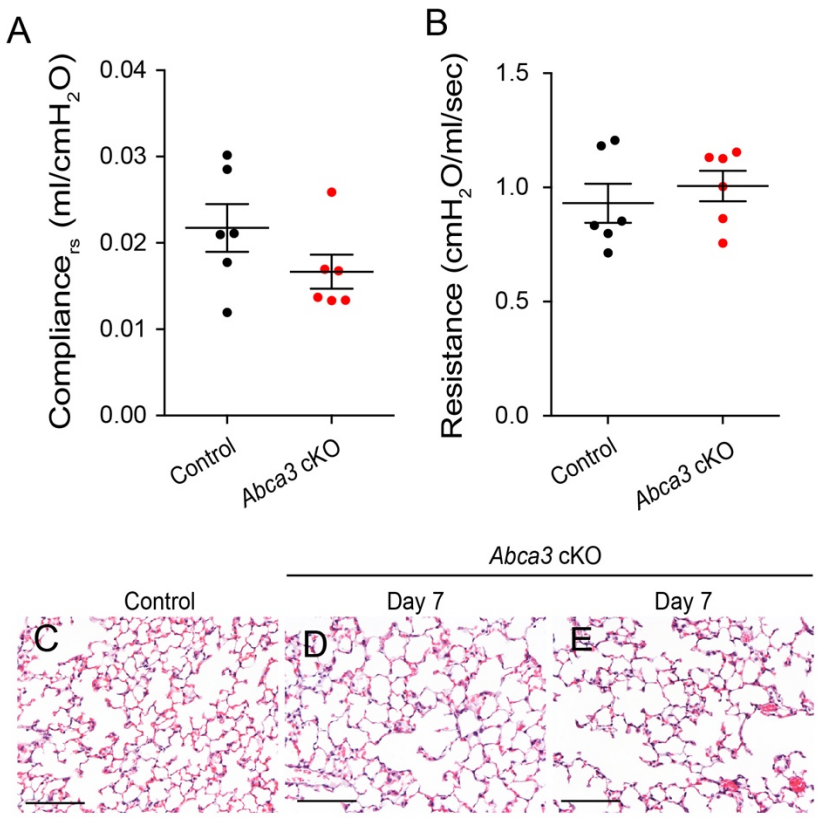

Fig. S6. Histological and physiological lung function is maintained 7 days following the loss of *Abca3*. Baseline tissue compliance (**A**) and elastance (**B**) in control and *Abca3* cKO mice treated with tamoxifen for 7 days. Data represent mean ± SE, n=6. Representative lung sections from control (**C**) and *Abca3* cKO mice (**D** and **E**) are shown. Scale bars = 100 μm.

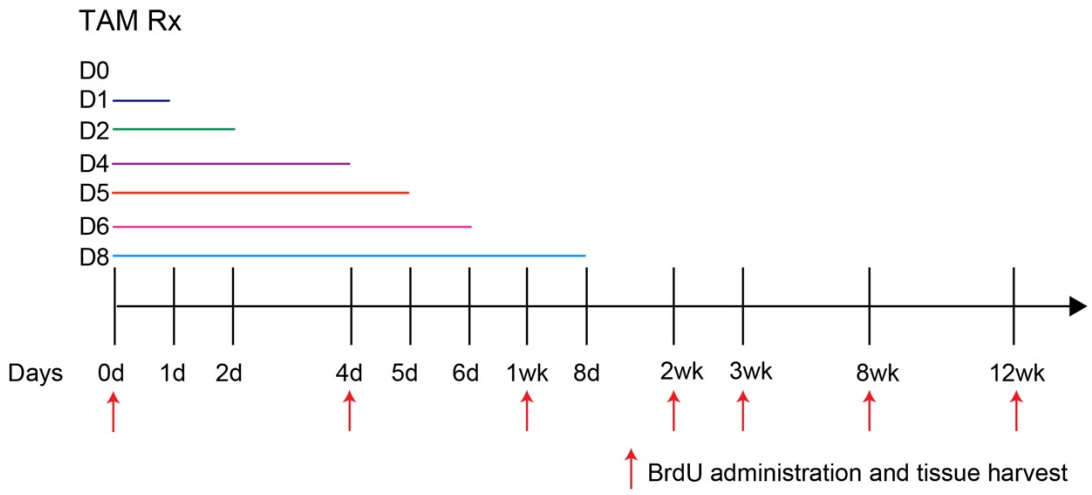

Fig. S7. Partial deletion model of *Abca3*. Schematic showing the timing of tamoxifen treatment (tamoxifen food) for 1-8 days (TAM Rx) followed by return to normal diet. Red arrows indicate timing of BrdU injection 2hrs prior to harvest at respective time points.

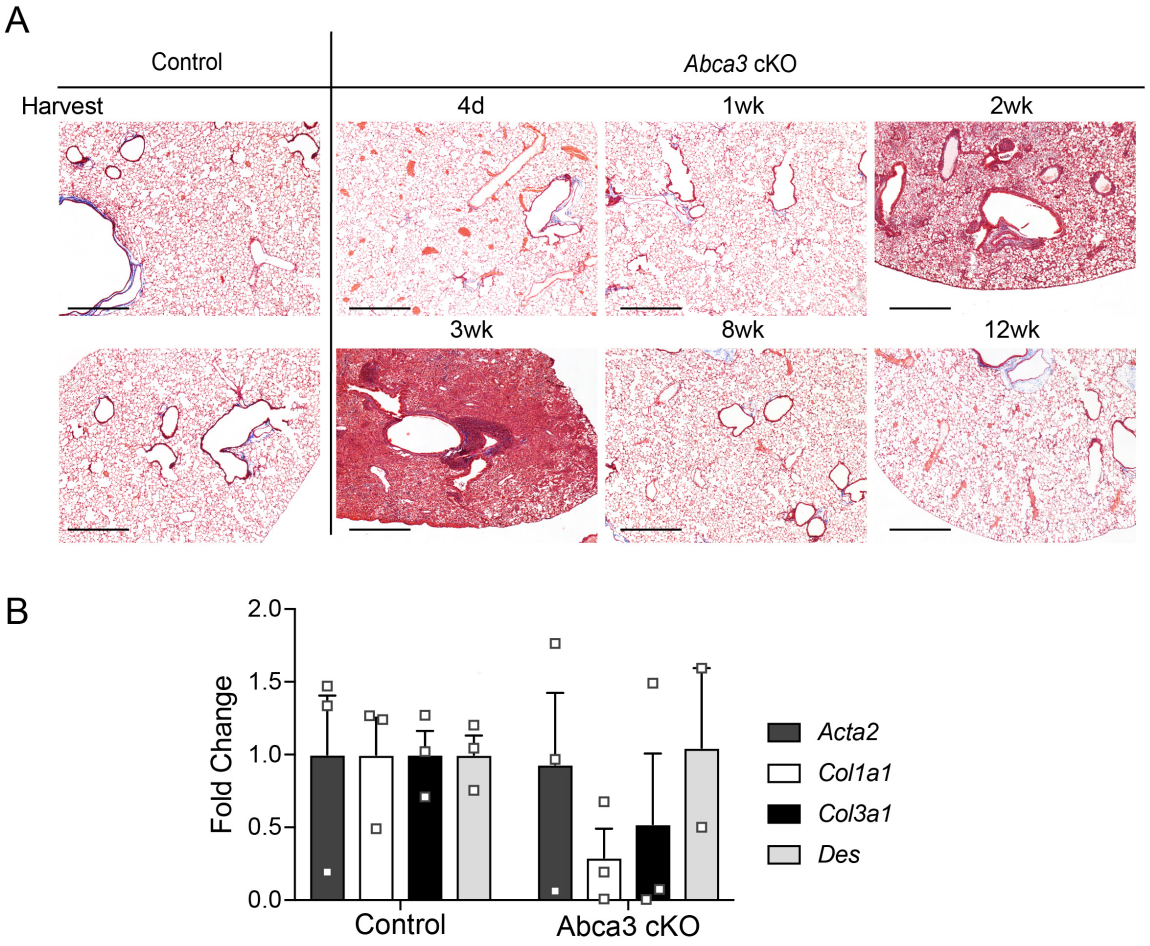

Fig. S8. Absence of fibrosis in regions of alveolar repair in *Abca3* cKO. A) Representative lung histology from control and *Abca3* cKO mice treated with tamoxifen for 4-days with tissue harvest at 4 days to 12 weeks. Lung tissue from n=3-4 mice/group were stained by Mason's trichrome for histological fibrotic analysis, scale bars, 500 μm. **B)** *Acta2*, *Col1a1*, *Col3a1*, and *Des* were measured by RT-PCR in whole lung from control and 12 week *Abca3* cKO mice. Data represent *Acta2*, *Col1a1*, *Col3a1*, and *Des* mRNA expression with dot plot overlay, n=2-3 mice/group.

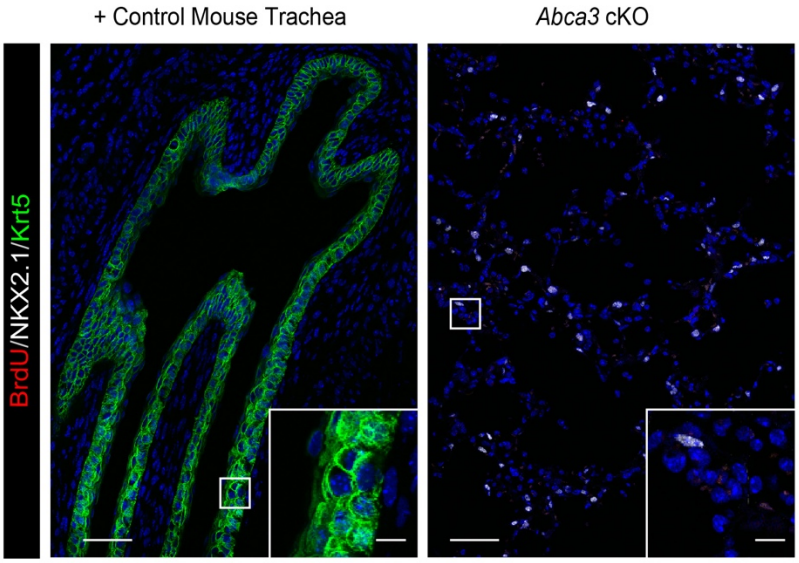

<u>Fig. S9.</u> Absence of Krt5 staining in regions of alveolar repair in *Abca3* cKO. Representative widefield tile scans of Krt5 (green), NKX2.1 (white), and BrdU (red) in mouse trachea (+ control) and *Abca3* cKO. n = 4, scale bars = 50 μm, inset scale bars = 10 μm.

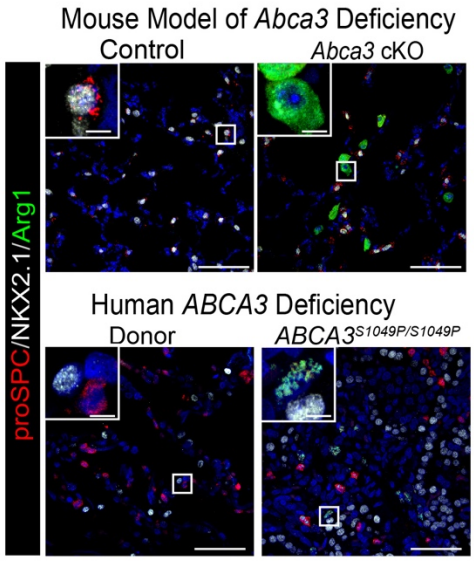

Fig. S10. Presence of M2-like macrophages in mouse models following partial loss of *Abca3* and human patients with *ABCA3* deficiency. Confocal immunofluescence for proSPC (red), NKX2.1 (white), and M2-like macrophages (ARG1, green) in *Abca3* cKO and human patients with ABCA3 deficiency. Scale bars = 50 μm, inset scale bars = 5 μm, n=3.

Table S1. Lipid species differentially regulated in *Abca3* cKO.

Phosphatidylcholine Species+A2:B146	Fold Change
PC(16:0/16:0) or DPPC	-1.704
PC(18:0/22:4)	-1.909
PC(16:0/16:4)	-2.000
PC(16:0/22:4)	-2.327
PC(18:1/20:1)	-2.446
PC(20:4/22:0)	-2.719
PC(18:1/24:0)	-2.790
PC(18:2/24:0)	-2.838
PC(18:0/22:5)	-2.890
PC(15:0/16:0)	-3.009
PC(14:0/16:0)	-3.092
PC(19:0/22:6)	-3.098
PC(18:1/24:1)	-3.138
PC(18:1/22:5)	-3.191
PC(18:0/20:4)	-3.197
PC(16:0/18:1);PC(16:1/18:0)	-3.203
PC(16:0/22:5);PC(18:1/20:4)	-3.222
PC(15:0/20:4)	-3.244
PC(20:3/22:0);PC(20:1/22:2)	-3.282
PC(17:0/20:4)	-3.309
PC(P-16:0/16:0)	-3.351
PC(16:0/16:1)	-3.418
PC(18:2/22:0)	-3.446
PC(18:0/20:3)	-3.451
PC(17:0/22:6)	-3.484
PC(16:0/24:0)	-3.493
PC(16:0/24:1);PC(18:1/22:0)	-3.497
PC(18:1/22:6)	-3.507
PC(16:0/20:4)	-3.533
PC(18:0/22:3)	-3.793
PC(16:0/20:1);PC(18:0/18:1)	-3.893
PC(19:0/20:4)	-3.932
PC(14:0/14:1)	-4.000
PC(16:1/18:1);PC(16:0/18:2)	-4.059
PC(18:0/22:5)	-4.091
PC(18:0/18:2)	-4.098
PC(18:1/22:1)	-4.186
PC(16:0/20:3)	-4.318
PC(14:0/22:6)	-4.569
PC(18:2/22:6)	-4.737
PC(16:0/17:0)	-4.860
PC(17:0/18:1)	-4.940
PC(16:0/O-16:0)	-5.007
PC(18:2/22:5)	-5.146
PC(16:0/18:0)	-5.709
PC(15:0/22:6)	-5.866
PC(18:2/20:4)	-5.886
PC(16:0/18:3)	-6.100
PC(16:0/17:1)	-6.323
PC(20:4/22:6)	-7.036
PC(14:0/15:0)	-7.149
PC(18:1/18:2)	-7.152
PC(15:0/18:2)	-7.257
PC(17:1/18:2)	-9.021
PC(18:2/18:2)	-9.605
PC(16:1/22:6)	-9.807
PC(16:1/20:4)	-10.265
PC(14:0/16:1)	-10.517
PC(16:1/18:2);PC(16:0/18:3)	-10.584
PC(15:1/16:0);PC(15:0/16:1)	-11.443
PC(16:0/20:5)	-12.108
PC(14:0/14:0)	-12.726
PC(16:0/18:3);PC(16:1/18:2)	-13.280
PC(16:0/18:4);PC(14:0/20:4)	-13.338
PC(14:0/18:2) ;PC(16:1/16:1) ;PC(16:2/16:0)	-15.588
PC(16:1/18:2)	-16.758
PC(16:3/16:0)	-19.134

Phosphatidylglycerol Species	Fold Change
PG(15:0/16:0)	-2.010
PG(16:0/18:2);PG(16:1/18:1)	-2.248
PG(16:0/20:4)	-3.238
PG(16:0/18:0)	-3.378
PG(16:0/16:0)	-3.635
PG(16:0/18:1);PG(16:1/18:0)	-3.660
PG(18:1/20:4)	-3.807
PG(17:0/18:2);PG(17:1/18:1)	-3.919
PG(16:0/16:1) ;PG(14:0/18:1)	-4.177
PG(16:0/16:1)	-4.501
PG(16:0/22:6)	-4.613
PG(20:5/22:6)	-4.754
PG(15:0/16:0)	-4.886
PG(18:1/22:6)	-5.347
PG(18:2/20:4)	-5.493
PG(18:1/18:2)	-5.771
PG(18:2/22:6)	-5.803
PG(16:0/17:0)	-5.975
PG(18:1/22:6)	-6.445
PG(16:1/22:6)	-6.559
PG(15:0/18:1);PG(16:0/17:1)	-6.838
PG(16:0/18:2)	-7.091
PG(18:2/18:2)	-7.407
PG(18:0/18:1)	-7.431
PG(14:0/16:0)	-7.669
PG(18:1/22:0)	-7.783
PG(18:2/22:4)	-7.791
PG(16:0/22:4)	-8.140
PG(18:0/22:6)	-8.669
PG(17:0/20:4)	-9.591
PG(18:0/22:6)	-9.876
PG(16:0/20:3)	-10.056
PG(18:1/18:2)	-10.404
PG(18:2/18:3)	-10.867
PG(16:1/18:2)	-11.137
PG(16:0/18:3);PG(16:1/18:2)	-11.346
PG(16:0/22:6)	-11.873
PG(16:0/20:4);PG(18:2/18:2)	-11.932
PG(17:1/18:2)	-12.459
PG(16:0/20:2);PG(18:1/18:1) ;PG(18:0/18:2)	-13.199
PG(15:0/18:2)	-17.044
PG(16:0/20:5);PG(16:1/20:4)	-21.812
PG(18:0/20:4)	-22.003
PG(16:1/16:1)_A;PG(14:0/18:2)	-24.969
PG(15:0/16:1)	-25.001
PG(16:1/22:6)	-29.287
PG(16:1/18:3)	-30.320
PG(16:1/16:1)_B;PG(16:2/16:0)	-32.972
PG(14:1/16:0)	-35.693
PG(14:1/16:0);PG(14:0/16:1)	-39.380
PG(14:0/14:0);PG(12:0/16:0)	-41.429
PG(16:3/16:0)	-44.221
PG(14:1/16:0)	-59.765
PG(16:1/20:4)	-70.327

Phosphatidylinositol Species	Fold Change
PI(18:0/20:3)	6.225
PI(16:0/18:2);PI(16:1/18:1)	1.953
PI(16:0/16:1)	-1.892
PI(16:0/18:3)	-2.311
PI(16:0/20:5)	-3.703
PI(18:2/20:4)	-5.537

Diacylglycerol Species	Fold Change
DG(18:0/18:1/0:0)	-3.692
DG(18:1/0:0/18:1)	-5.332
DG(16:0/0:0/16:0)	-5.697
DG(14:0/16:0/0:0)	-7.683
DG(16:0/20:4/0:0)	-12.006
DG(16:0/18:1/0:0)	-12.554
DG(16:0/22:5/0:0);DG(18:1/20:4/0:0)	-12.933
DG(16:0/22:6/0:0)	-13.569
DG(16:1/18:2/0:0)	-14.493
DG(16:0/16:1/0:0)	-18.325
DG(16:0/20:5/0:0)	-20.766

Table S2. Primer and Antibodies

Genotyping Primers	Forward	Reverse
mouse *Abca3*	5'-AGC ACT TTT CCC TCT CTG GCC TTG AG-3'	5'-TGC CCA CCC AGC ACC ATG CT-3'
Sftpc-CreER^{T2}	5'-ATG GGA TCT GAT CTG GGG-3'	5'-TTC AAC TTG CAC CAT GCC-3'
tdTomato Wildtype	5'-AAG GGA GCT GCA GTG GAG TA-3'	5'-CCG AAA ATC TGT GGG AAG TC-3'
tdTomato Mutant	5'-GGC ATT AAA GCA GCG TAT CC-3'	5'-CTG TTC CTG TAC GGC ATG G-3'

Immunofluescence Antibody	Species	Cat#/Company	Diltion
ARG1	Sheep (FITC, no secondary)	IC5868F; R&D Systems	1:50
ABCA3	rabbit polyclonal	WRAB-70565; Seven Hills Bioreagents	1:100
ABCA3	guinea pig polyclonal	GP985, in house	1:100
proSPC	goat polyclonal	SC-7706; Santa Cruz	1:100
proSPC	guinea pig polyclonal	GP992, in house	1:100
proSPC	rabbit polyclonal	WRAB-9337, Seven Hills Bioreagents	1:100
proSPB	rabbit polyclonal	WRAB-55522; Seven Hills Bioreagents	1:100
CD45	goat polyclonal	AF114; R&D Systems	1:100
SOX2	rabbit polyclonal	R1236; Seven Hills Bioreagents	1:200
HOPX	rabbit polyclonal	SC-30216; Santa Cruz	1:200
KRT5	rabbit polyclonal	PRB-160-200; Biolegend	1:200
ECAD	rabbit polyclonal	24E10; Cell Signaling Technology	1:300
NKX2.1	guinea pig polyclonal	G237; in house	1:500
BrdU	rat polyclonal	ab6326; abcam	1:50
BrdU	mouse monoclonal IgG1	G3G4; Hybridoma Bank University of Iowa	1:500
CD206	rat polyclonal	MCA2235T; AbD Serotec	1:1,000

AT2 Isolation Antibodies	Cat#
CD45	BioLegend, 103103
CD16/32	BD Bioscience, 553143
Ter119	BioLegend, 116203
CD90	BioLegend, 105304
CD31	BioLegend, 102503

Taqman Probes	Cat#
Abca3 exons 3-4	Mm00550480_g1
Abca3 exons 5-6	Mm01299927_g1
Arg1	Mm00475988_m1
Retnla	Mm00445109_m1
Mrc1	Mm01329362_m1
ACTB	Applied Biosystems, 4352663
18S	Applied Biosystems, 4352930
Acta2	Mm00725412_s1
Col1a1	MM00801666_g1
Col3a1	Mm00802331_m1
Des	MM00802455_m1

FACs Antibody	Cat#/Company
Live/Dead Zombie UV	423107, BioLegend
pan CD45 (clone 30-F11) PE-Dazzle 594	103145, BioLegend
F4/80 APC	123115, BioLegend
CD11b PE	101207, BioLegend
CD11b PE	557397, BD Bioscience
Ly-6G Pacific Blue	127611, BioLegend
CD11c PerCP/Cy5.5	117327, BioLegend

Table S3. **Human *ABCA3* Deficiency**

Human *ABCA3* mutations	Tissue Source
MC1553P/L1553P	surgical biopsy
W1142X/W1142X	surgical biopsy
L982P/G1221S	surgical biopsy
Q1591P/Q1131R	surgical biopsy
S1049P/S1049P	expant tissue